Molecular Pharmacology Fast Forward. Published on December 13, 2006 as doi:10.1124/mol.105.021683
This article has not been copyedited and formatted. The final version may differ from this version.

MOL 21683

Analysis of mammalian carboxylesterase inhibition by trifluoromethylketone-containing compounds

Randy M. Wadkins, Janice L. Hyatt, Carol C. Edwards, Lyudmila Tsurkan, Matthew R. Redinbo, Craig E. Wheelock*, Paul D. Jones, Bruce D. Hammock and Philip M. Potter

Department of Chemistry and Biochemistry, University of Mississippi, University, MS 38677 (R.M.W.);

Department of Molecular Pharmacology, St. Jude Children's Research Hospital, Memphis, TN 38105 (J.L.H., C.C.E., L.T., P.M.P);

Department of Chemistry, University of North Carolina at Chapel Hill, Chapel Hill, NC 27599 (M.R.R.);

Department of Entomology, and Cancer Research Center, University of California Davis, Davis, CA 95616 (C.E.W., P.D.J., B.D.H.).

* Current address: Microbiology and Tumor Biology Center, Karolinska Institute, Nobels väg 16, SE-171 77 Stockholm, Sweden.

Molecular Pharmacology Fast Forward. Published on December 13, 2006 as DOI: 10.1124/mol.105.021683
This article has not been copyedited and formatted. The final version may differ from this version.

MOL 21683

Running title: Inhibition of carboxylesterases by trifluoromethylketones

Corresponding author:

Dr. Philip M. Potter,

Department of Molecular Pharmacology,

St. Jude Children's Research Hospital,

332 N. Lauderdale,

Memphis, TN 38105-2794,

Tel: 901-495-3440;

Fax: 901-495-4293;

E-mail: phil.potter@stjude.org

Text pages:	43 (including tables)
Number of tables:	6
Number of figures:	4
Number of references:	40
Number of words -	
Abstract:	249
Introduction:	747
Discussion:	1499

Abbreviations: AChE - acetylcholinesterase; c - competitive enzyme inhibition; CE - carboxylesterase; CPT-11 - irinotecan; DMSO - dimethyl sulfoxide; hAChE - human AChE; hBChE - human butyrylcholinesterase; hCE1 - human carboxylesterase 1;

Molecular Pharmacology Fast Forward. Published on December 13, 2006 as DOI: 10.1124/mol.105.021683
This article has not been copyedited and formatted. The final version may differ from this version.

hiCE - human intestinal carboxylesterase; K_i - inhibition constant.; K_{iapp} – apparent K_i values; *i* = fractional inhibition; Mp - melting point; nc - non-competitive enzyme inhibition; o-NPA - o-nitrophenyl acetate; pc - partially competitive enzyme inhibition; pnc - partially non-competitive enzyme inhibition; q^2 - cross correlation coefficients; QSAR - quantitative structure activity relationship; rCE - rabbit liver carboxylesterase; TFK - trifluoromethyl ketone; v_o = initial enzyme velocity in the absence of inhibitor.

Molecular Pharmacology Fast Forward. Published on December 13, 2006 as DOI: 10.1124/mol.105.021683
This article has not been copyedited and formatted. The final version may differ from this version.

Abstract

Carboxylesterases (CE) are ubiquitous enzymes that hydrolyze numerous ester-containing xenobiotics including complex molecules such as the anticancer drugs, CPT-11 and capecitabine, and the pyrethroid insecticides. Due to the role of CEs in the metabolism of many exogenous and endogenous ester-containing compounds, a number of studies have examined the inhibition of this class of enzymes. Trifluoromethylketone-containing (TFK) compounds have been identified as potent CE inhibitors. In this article, we present inhibition constants for 21 compounds, including a series of sulfanyl, sulfinyl and sulfonyl TFKs with 3 mammalian CEs, as well as human acetyl- and butyrylcholinesterase. In order to examine the nature of the slow tight-binding inhibitor/enzyme interaction, assays were performed using either a 5 min or a 24 hour preincubation period. Results showed that the length of the preincubation interval significantly affects the inhibition constants on a structurally-dependent basis. The TFK-containing compounds were generally potent inhibitors of mammalian CEs, with K_i values as low as 0.3 nM observed. In most cases, thioether-containing compounds were more potent inhibitors then their sulfinyl or sulfonyl analogs. QSAR analyses demonstrated excellent observed versus predicted values correlations (r^2 ranging from 0.908 - 0.948) with cross correlation coefficients (q^2) of ~0.9. In addition, pseudoreceptor models for the TKF analogs were very similar to structures and models previously obtained using benzil- or sulfonamide-based CE inhibitors. These studies indicate that more potent, selective CE inhibitors, containing long alkyl or aromatic groups attached to the thioether chemotype in TFKs, can be developed for use in *in vivo* enzyme inhibition.

INTRODUCTION

Carboxylesterases (CE) have been identified in organisms ranging from bacteria to humans and are thought to be responsible for the detoxification of xenobiotics (Cashman et al., 1996). CEs (EC 3.1.1.1) are members of the α/β hydrolase family and cleave carboxylesters (RCOOR') into the corresponding carboxylic acid (RCOOH) and alcohol (ROH) via a proton transfer hydrolysis mechanism using a catalytic serine present within a Ser-His-Glu triad (Redinbo and Potter, 2005). These enzymes metabolize numerous clinically useful drugs (e.g. CPT-11, capecitabine, meperidine) as well as the illicit compounds heroin and cocaine, and commercial pesticides (e.g. permethrin, malathion) (Ahmad and Forgash, 1976; Potter et al., 1998; Ross et al., 2006; Wheelock et al., 2005). Consequently, the development of specific CE inhibitors may have both therapeutic, as well as commercial, utility (Ashour and Hammock, 1987; Hammock et al., 1982; Linderman et al., 1989).

Some of the most potent CE inhibitors identified to date are a group of compounds collectively known as trifluoromethyl ketones (TFKs; $RCOCF_3$). These compounds contain a trifluoromethyl group in the α position with respect to the ketone moiety (Figure 1). The trifluoroacyl chemotype is very efficient at inhibiting enzymes whose catalytic mechanism involves attack by a nucleophilic catalytic residue (e.g. serine). The resulting tetrahedral TFK adduct contains: the trifluoromethyl group; the protein (via the serine residue); a $C-O^-$ oxyanion, (from the ketone oxygen); and the respective inhibitor moiety (e.g. an alkyl chain). However, as the trifluoromethyl group is a poor leaving group, the enzyme is reversibly inhibited. The extreme

Molecular Pharmacology Fast Forward. Published on December 13, 2006 as DOI: 10.1124/mol.105.021683
This article has not been copyedited and formatted. The final version may differ from this version.

potency of these compounds is attributed to the polarization of the carbonyl by the trifluoromethyl group, which greatly increases the electrophilicity of the carbonyl carbon and hence its susceptibility to nucleophilic attack (Székács et al., 1992). Of particular interest is the observation that in TFK-containing inhibitors or in more broadly polarized ketones, the polarization of the carbonyl group shifts the equilibrium towards the *gem*-diol form (Figure 1) (Roe et al., 1997).

TFKs were first studied as inhibitors of acetylcholinesterase (AChE; (Brodbeck et al., 1979)). Shortly thereafter, a number of articles described the use of the TFK moiety as an inhibitor of esterases, including juvenile hormone esterase (Hammock et al., 1984; Hammock et al., 1982), and mammalian enzymes (Ashour and Hammock, 1987). The large number of TFK-containing CE inhibitors reported in the literature has been extensively analyzed via quantitative structure activity relationship (QSAR) techniques using juvenile hormone esterase (Rosell et al., 1996; Székács et al., 1992; Wheelock et al., 2002; Wheelock et al., 2003). In general, the potency of the aliphatic TFKs exhibits a strong positive correlation with lipophilicity; however, inhibitor potency can be increased by specific substitutions that do not strongly affect the overall lipophilicity or shape of the inhibitor. This correlation breaks down with branched chain or cyclic compounds, and it has also been shown that increasing the degree of fluorination increases inhibitor efficacy (Székács et al., 1992).
Further research using TFK-containing compounds showed that substitution of the β-carbon with a sulfur atom (Figure 1) led to a significant increase in inhibitor potency (Ashour and Hammock, 1987; Hammock et al., 1984). The sulfur atom was

Molecular Pharmacology Fast Forward. Published on December 13, 2006 as DOI: 10.1124/mol.105.021683
This article has not been copyedited and formatted. The final version may differ from this version.

initially incorporated into TFK inhibitors to serve as a bioisostere of the olefin group in juvenile hormone. However, the resulting increase in compound efficacy was greater than expected, and led to alternative hypotheses regarding the role of the sulfur atom (Székács et al., 1992). Potentially, this atom may be involved in intramolecular hydrogen bonding with the ketone and/or *gem*-diol (Székács et al., 1992), thereby shifting the equilibrium towards the latter form. Alternatively, the sulfur may be involved in π-orbital stacking or other interactions with amino acid residues within the enzyme active site (Wheelock et al., 2002). A recent study has elucidated some of the physical interactions that the sulfur atom undergoes in juvenile hormone esterase; however the effects upon mammalian enzymes are still unclear.

In this article, we have examined the inhibition of three recombinant mammalian CEs by a series of TFKs and determined 3D-QSAR pseudoreceptor models that account for their biological activity. These results demonstrate not only that differences in inhibitor structure affect enzyme inhibition (e.g. the length of the alkyl chain), but also that subtle differences within the CE active sites significantly influences the potency of these compounds. These data will be of particular use in comparing differences between insect and mammalian CE structure activity relationships. In addition, these inhibitors may also prove useful for elucidating the endogenous role of these enzymes, or for affinity purification of esterases and related enzymes.

Molecular Pharmacology Fast Forward. Published on December 13, 2006 as DOI: 10.1124/mol.105.021683
This article has not been copyedited and formatted. The final version may differ from this version.

MATERIAL AND METHODS

Enzyme and inhibitors

hCE1 and rCE were purified as previously described (Morton and Potter, 2000). hiCE was purified in a similar manner, however the enzyme was only about 50% pure. Contaminating proteins in this sample included BSA and baculoviral proteins that have been shown not to affect kinetic studies with this enzyme (Wadkins et al., 2004). The Genbank accession numbers for the cDNAs encoding the CEs used in these studies were as follows; hiCE - Y09616 (Schwer et al., 1997); hCE1 - M73499 (Munger et al., 1991); and rCE - AF036930 (Potter et al., 1998).

hAChE and hBChE were obtained from Sigma Biochemicals (St. Louis, MO).

The ether, sulfanyl and sulfonyl TFK inhibitors (Table 1) were synthesized as previously described (Wheelock et al., 2002; Wheelock et al., 2001). Compound **7**, (1,1,1-trifluorododecan-2-one), was synthesized according to the methods of Hammock et al (Hammock et al., 1982). Compounds were characterized by ^{1}H NMR and MS and all data were in agreement with previously published values. The structures of all compounds tested are shown in Table 1. Inhibitors are shown as either the ketone or hydrate based upon the presence of a *gem*-diol signal by ^{1}H NMR (2 broad downfield singlets when acquired in $CDCl_3$). Inhibitors were dissolved in DMSO immediately before use.

Synthesis of 1,1,1-trifluoro-3-(alkylsulfinyl)propane-2,2-diols

The 1,1,1-trifluoro-3-(alkylsulfinyl)propane-2,2-diols (alkyl TFK sulfoxides) were synthesized via the same general procedure as the above compounds. To the corresponding thioether (1 eq) in dichloromethane (conc. = 0.1 M) at 0^{o}C was added

Molecular Pharmacology Fast Forward. Published on December 13, 2006 as DOI: 10.1124/mol.105.021683
This article has not been copyedited and formatted. The final version may differ from this version.

m-chloroperoxybenzoic acid (1eq). The reaction was stirred overnight, washed with 1M K_2CO_3 and the organic layer dried with Na_2SO_4. After filtering, the solvent was removed under reduced pressure and the target compound was recovered by recrystallization from dichloromethane/hexane in 30 – 35% yield. Physical parameters of the compounds are indicated below.

1,1,1-trifluoro-3-(butylsulfinyl)propane-2-2-diol

^{1}H (300 MHz, $CDCl_3$): 6.37 (br, 1H), 5.17 (br, 1H), 4.20 – 4.00 (m, 0.3 H), 3.20 – 2.80 (m, 4H), 1.90 – 1.70 (m, 2H), 1.60 – 1.40 (m, 2H), 0.99 (t, *J* = 0.97 Hz, 3H); Mp = 79 - 82 ^{o}C.

1,1,1-trifluoro-3-(hexylsulfinyl)propane-2-2-diol

^{1}H (300 MHz, $CDCl_3$): 6.34 (br, 1H), 4.76 (br, 1H), 4.15 – 4.00 (m, 0.4 H), 3.15 – 2.80 (m, 4H), 1.90 – 1.70 (m, 2H), 1.60 – 1.25 (m, 6H), 0.89 (m, 3H); Mp = 89 - 91 ^{o}C.

1,1,1-trifluoro-3-(octylsulfinyl)propane-2-2-diol

^{1}H (300 MHz, $CDCl_3$): 6.36 (br, 1H), 4.88 (br, 1H), 4.15 – 4.00 (m, 0.16 H), 3.15 – 2.80 (m, 4H), 1.90 – 1.70 (m, 2H), 1.60 – 1.25 (m, 10H), 0.89 (m, 3H); Mp = 87 - 90 ^{o}C.

1,1,1-trifluoro-3-(decylsulfinyl)propane-2-2-diol

^{1}H (300 MHz, $CDCl_3$): 6.35 (br, 1H), 4.76(br, 1H), 4.17 – 4.00 (m, 0.16 H), 3.20 – 2.80 (m, 4H), 1.90 – 1.70 (m, 2H), 1.60 – 1.25 (m, 14H), 0.88 (m, 3H); Mp = 90 - 95 ^{o}C.

1,1,1-trifluoro-3-(dodecylsulfinyl)propane-2-2-diol

Molecular Pharmacology Fast Forward. Published on December 13, 2006 as DOI: 10.1124/mol.105.021683
This article has not been copyedited and formatted. The final version may differ from this version.

^{1}H (300 MHz, $CDCl_3$): 6.32 (br, 1H), 4.70(br, 1H), 4.20 – 4.00 (m, 0.05 H), 3.20 – 2.80 (m, 4H), 1.90 – 1.70 (m, 2H), 1.60 – 1.25 (m, 18H), 0.86(m, 3H); Mp =98 – 100^{o}C.

Predicted water solubilities and logP values of inhibitors

Water solubilities and logP values were predicted using ChemSilico Predict v2.0 software (ChemSilico LLC, Tewksbury, MA).

Carboxylesterase inhibition

Inhibition of CEs was assessed using 3 mM *o*-nitrophenyl acetate (o-NPA) as a substrate in 50mM Hepes pH7.4 over a 5 minute time period (Wadkins et al., 2005; Wadkins et al., 2004). Inhibitor was added either simultaneously with o-NPA or after a 24 hr preincubation (in the absence of substrate). Routinely, assays were performed in duplicate in multiwell plates using at least 8 concentrations of inhibitor, ranging from 1 pM to 100 μM. Positive (50 μM bis-4-nitrophenyl phosphate) and negative (DMSO) controls were included in all assays.

Acetylcholinesterase and butyrylcholinesterase inhibition

Inhibition of hAChE and hBChE was assessed using multiwell plate assays as previously described (Doctor et al., 1987; Morton et al., 1999; Wadkins et al., 2005; Wadkins et al., 2004; Wadkins et al., 1999).

Analysis of enzyme inhibition

To determine the K_i values and the mode of enzyme inhibition, data were fitted to the following equation (Webb, 1963; see scheme 1):

$$i = \frac{[I]\{[S](1-\beta) + Ks(\alpha-\beta)\}}{[I]\{[S] + \alpha Ks\} + Ki\{\alpha[S] + \alpha Ks\}} \qquad \text{(Eq.1)}$$

Molecular Pharmacology Fast Forward. Published on December 13, 2006 as DOI: 10.1124/mol.105.021683
This article has not been copyedited and formatted. The final version may differ from this version.

where i = fractional inhibition, [I] = inhibitor concentration, [S] = substrate concentration, α = change in affinity of the substrate for the enzyme in the presence of the inhibitor, β = change in the rate of enzyme substrate complex decomposition in the presence of the inhibitor, K_s is the dissociation constant for the enzyme substrate complex (assuming negligible commitment to catalysis) and K_i is the inhibitor constant. The data sets were analyzed using GraphPad Prism software and Perl Data Language, and the mode of enzyme inhibition was determined by evaluating the r^2 values for the curve fits using Akaike's information criteria (Wadkins et al., 2005). K_i values were then calculated using the best fit model described from these analyses.

In most cases, enzyme inhibition was either partially competitive (i.e. where the inhibitor does not affect the rate of enzyme/substrate complex dissociation and only partially hinders substrate binding) or partially non-competitive (i.e. were the binding of substrate to the enzyme is unaffected by the inhibitor, but the dissociation of the enzyme/inhibitor/substrate complex is slower than that of the enzyme/substrate complex).

Analysis of datasets obtained from preincubation of the enzyme with the inhibitor for 24 hours indicated, that in some instances, the 'on' rate for the small molecules was very slow (and/or that the formation of enzyme/inhibitor complex occurred slowly). Since equation 1 cannot yield accurate K_i values from the preincubation studies, we determined apparent inhibition constants (K_{iapp}) using this equation and also reanalyzed the datasets using the approaches described previously (Morrison and

Molecular Pharmacology Fast Forward. Published on December 13, 2006 as DOI: 10.1124/mol.105.021683
This article has not been copyedited and formatted. The final version may differ from this version.

Walsh, 1988). These take into consideration the slow binding of inhibitors in the absence of substrate.

Analyses of the inhibitor concentration effect on initial velocities (v_o) of substrate conversion typically showed the characteristic pattern of a "mechanism B" type inhibitor. This type of inhibitor has been extensively reviewed (Morrison and Walsh, 1988), and is described by the mechanism of Webb (Webb, 1963), except that the EIS complex is not formed, and the inhibitor forms a new isomer species (EI*) that can to revert to the EI complex. Under these conditions, the inhibition of initial velocities (v_o) is given by:

$$v_o = \frac{V_{\max}[S]}{K_M(1+\frac{[I]}{K_i})+[S]} \qquad \text{(Eq.2)}$$

where K_M is determined in the absence of inhibitor, [I] is the inhibitor concentration, [S] is the substrate concentration, and V_{max} is the maximum velocity achieved in the presence of the inhibitor. This equation holds true where the conversion from EI* to EI is rapid, relative to the reverse reaction.

Molecular modeling of inhibitors of carboxylesterase

3D-QSAR analyses were performed using Quasar 5.0 (Stewart, 1990; Vedani and Dobler, 2002a; Vedani and Dobler, 2002b; Vedani et al., 2005) running on a Macintosh G4. Structures for each analog were initially constructed with Chem3D for Macintosh using the compounds shown in Table 1 (i.e. compound **1** was constructed as the ketone and compound **2** as the *gem*-diol). Partial atomic charges from the bond charge correction method (Jakalian et al., 2002) and AMBER atom types were assigned using the *antechamber* module of AMBER7 (University of California, San

Francisco, CA). Structures for QSAR analysis were performed by initial energy minimization of compound **4** using the PM3 Hamiltonian of MOPAC (Stewart, 1990). All analogs were then aligned using the decyl chain and the S-C-C=O dihedral of **4** as a template.

RESULTS

Inhibition of CE by TFKs and their structural analogs

To assess the ability of the TFKs to inhibit CEs, inhibition studies were performed using *o*-NPA as a substrate and K_i values for each inhibitor (Table 1) with each enzyme were determined. As indicated in Tables 2 and 3, the thioether TFKs (compounds **1**, **4**, **8**, **11**, **18** and **20**) were all potent inhibitors of the 3 different mammalian CEs, with K_i values ranging from 0.3 to 1670 nM. For the 5 minute data sets (Table 2), the potency of enzyme inhibition was clearly related to the length of the alkyl chain. For example, the butyl derivative (**18**) was ~100-fold less potent against hiCE as compared to the dodecyl analog (**1**) with the intermediate length molecules falling within this range. Plots of the data sets comparing the K_i values with the number of carbon atoms in the alkyl moiety yielded linear relationships (Figure 2A). The r^2 values for these curve fits were 0.937, 0.981 and 0.754 for hiCE, hCE1 and rCE, respectively. Interestingly, the change in potency afforded by the alkyl group was much more pronounced in hiCE as compared to rCE, as evident by the differences in the slopes of the lines in Figure 2.

However, similar analyses using the data derived from the 24 hr inhibition assays (Table 3), did not yield such relationships, with r^2 values ranging from 0.07 - 0.1 (data not shown). These results suggest that it is the initial interaction of the inhibitor and the enzyme that is modulated by the alkyl chain length.

In the short duration assays (5 min), the sulfinyl *gem*-diol TFKs ($RS(O)CH_2C(OH)_2CF_3$; compounds **2**, **5**, **9**, **12**, and **19**) were all weaker CE inhibitors. This trend was also dependent upon alkyl chain length. For example, with

Molecular Pharmacology Fast Forward. Published on December 13, 2006 as DOI: 10.1124/mol.105.021683
This article has not been copyedited and formatted. The final version may differ from this version.

hiCE, compounds with long alkyl chains (e.g. **2)**, only exhibited a ~3.5-fold reduction in potency relative to the thioether analog (**1**). However, the shorter chain analog (**12**) showed a ~120-fold reduction in potency (Table 1). In addition, the butyl derivative (**19**) was inactive against all the enzymes examined in this assay system. In general, these sulfoxide-containing analogs were 10- to 30-fold weaker in their ability to inhibit CEs.

In contrast, in the 24 hour assays, the sulfinyl *gem*-diol TFKs were more potent at CE inhibition than the thioether analogs. For example, compound **5** demonstrated K_i values of 1.9, 5.3 and 2.5 μM for hiCE, hCE1 and rCE respectively, when assayed over 5 min. However, this same molecule displayed K_{iapp} values of 6.6, 0.5 and 16.1 nM after incubation with the same panel of enzymes for 24 hours. Hence for this compound, it is likely that the 'on' rate for the CEs is slow and that the equilibrium requires a considerable amount of time to be established.

The longer chain (C_8 - C_{12}) sulfonyl *gem*-diols ($RS(O_2)CH_2C(OH)_2CF_3$; compounds **3**, **6**, **10**, **13**, **16**, and **21**) were reasonably effective at CE inhibition in the 5 min assays, with K_i values ranging from 50 – 4700 nM. However in the 24 hour reactions, the inhibition constants were considerably reduced, with most values ranging from 0.59 – 376 nM. The exception was compound **16** were K_{iapp} values were considerable larger (450 – 18,300 nM).

As indicated earlier, it is likely that the "on/off" rate of the inhibitors would significantly affect substrate hydrolysis, especially under conditions where the enzyme had been preincubated with the compounds for extended periods of time. Therefore, we reanalyzed the 24 hr datasets using the model described by Morrison

Molecular Pharmacology Fast Forward. Published on December 13, 2006 as DOI: 10.1124/mol.105.021683
This article has not been copyedited and formatted. The final version may differ from this version.

and Walsh (Morrison and Walsh, 1988). Using this approach, we fitted the v_o data vs. inhibitor concentration using non-linear least-squares analysis to obtain K_i for the compounds (Table 4). In general, the values were similar to the pc and pnc data given in Table 3, indicating that both the general analysis and the more specialized slow-binding analysis could be used to interpret our inhibitor data. There are a few exceptions, notably compounds **7**, **16**, and **20**. Clearly, the K_i values obtained with these analogs are significantly dependent on the model chosen to fit the data. We have therefore provided both K_{iapp} and K_i values to acknowledge this point. Interestingly, some of the compounds demonstrated inhibitory activity towards both hAChE and hBChE. For example, compound **4** exhibited K_i values of ~700 nM and ~11 μM with hAChE and hBChE, respectively, after 5 min incubation. It is unclear why this particular compound, which has an alkyl chain consisting of 10 carbon atoms would be effective as an inhibitor, as compared to compounds **1** (C_{12}**)** and **8** (C_8). However, in general, inhibition of the cholinesterases was weak and only occurred at much higher inhibitors concentrations (typically > 10 μM).

Correlations between the K_i values and the ClogP or the water solubilities of the TFK inhibitors

As indicated above, the K_i values obtained from the 5 min assays were correlated with the length of the alkyl chain within the thioether TFK containing inhibitors (Figure 2A). Since the active sites of the mammalian CEs are lined with aromatic amino acids that create a highly hydrophobic domain within the protein, we hypothesized that the ClogP values and/or the water solubility of the compounds may also correlate with their inhibitory potency. Therefore, the ClogP values and the

Molecular Pharmacology Fast Forward. Published on December 13, 2006 as DOI: 10.1124/mol.105.021683
This article has not been copyedited and formatted. The final version may differ from this version.

water solubilities of the inhibitors were predicted from their chemical structures using ChemSilico Predict software (Table 5). Graphical plots of these datasets with the K_i values for the different enzymes are depicted in Figures 2B and 2C. Good correlations between these parameters were observed, consistent with previous results seen in Figure 2A. Since the length of the alkyl group, the hydrophobicity of the molecules, and the water solubility of the inhibitors are inversely related, it is perhaps, not surprising that there is a correlation with the inhibitory potency of these compounds. However, it is clear that these simple models may have some predictive power towards the design of novel TFK inhibitors.

As mentioned above, no correlations between these parameters were observed with the data obtained following preincubation of the inhibitor with the enzymes for 24 hr. This suggests that the initial interaction of the thioether TFKs with the CEs is modulated by the alkyl group, but over extended periods of time this effect is minimized.

Molecular modeling of TFK-mediated inhibition of CEs

To assess the contribution of the chemical properties of the molecules towards enzyme inhibition, 3D-QSAR analyses were performed using Quasar 5.0 software (Vedani and Dobler, 2002a; Vedani and Dobler, 2002b; Vedani et al., 2005). Only those analogs from Table 3 that displayed partial non-competitive (pnc) inhibition were used to generate the pseudoreceptor models. The K_i values predicted for the inhibitors that operate by other mechanisms were then compared.

The r^2 correlation coefficients for the predicted versus experimental K_i values for hiCE, hCE1, and rCE are shown in Figure 6 and Table 3. These results indicate that

Molecular Pharmacology Fast Forward. Published on December 13, 2006 as DOI: 10.1124/mol.105.021683
This article has not been copyedited and formatted. The final version may differ from this version.

the models obtained from these analyses are highly correlative. To determine whether these models may have predictive power for TFKs of unknown biological activity, the cross correlation coefficients (q^2) were calculated. These values were ~0.900 for all enzymes under both experimental conditions (Table 6). Again, these results suggest that the models would have considerable predictive power for TFKs with unknown biological activity. An alternative measure of the significance of these analyses is demonstrated in Table 6, which displays the q^2/r^2 values for the datasets. As indicated, these values are close to unity, suggesting that the models derived from these QSAR studies are highly correlative and predictive.

3D-QSAR pseudoreceptor models of TFK-mediated inhibition of CEs

Using the Quasar software, 3D pseudoreceptor models for the TFK analogs were generated from the inhibition data sets and the enzyme-ligand binding sites are shown in Figure 4. The 24 hr inhibition datasets were used for model construction as these conditions most likely offer a more accurate representation of the equilibrium established between enzyme and inhibitor. The pseudoreceptor models generated for the TFK analogs (Figure 4) are remarkably similar in structure to those obtained from the QSAR analysis of the previously characterized benzil- and sulfonamide-based CE inhibitors (Wadkins et al., 2005; Wadkins et al., 2004). These models accurately reflect the charged amino acid residues in the active site gorges of the CEs examined. Although it is impossible to assign a direction to the pseudoreceptor models, we anticipate that the orientation shown in Figure 4 has the entrance to the gorge at the top and the active site, containing the catalytic residues, at the bottom.

This is logical inasmuch as the bottom of the gorge contains charged residues while the central portion is lined with mostly hydrophobic residues.

The interpretation of the models in this manner is then straightforward with regard to the differential activities of the different inhibitors. For hCE1, less charge density is found near the bottom of the gorge than for the other CEs. Hence, compounds such as **7**, which contains a hydrophobic trifluoromethyl group and lacks an electron withdrawing carbonyl oxygen atom, inhibits hCE1 better than the other CEs. In contrast, the models more accurately predict the inhibition of hiCE and rCE by the TFK analogues, as depicted by the cationic areas present at the bottom of the active site gorge. These regions presumably facilitate hydrogen bonding of amino acids with the sulfinyl and sulfonyl oxygen atoms. However, as compared to the benzil analogs (Wadkins et al., 2005), the models for the different enzymes show more similarity to each other, with the putative active site (bottom of the figure) having the most significant differences. Consequently, the enzyme selectivity that was observed with the benzil analogues was not seen with the TFK compounds. In general, the ability of the models to fit the K_i data was good (Figure 3), indicating that they should allow for the accurate prediction of inhibitory potency and development of other TFK-containing compounds.

Molecular Pharmacology Fast Forward. Published on December 13, 2006 as DOI: 10.1124/mol.105.021683
This article has not been copyedited and formatted. The final version may differ from this version.

Discussion

In this study, we examined the ability of TFKs to inhibit human and rabbit CEs, and present detailed QSAR models describing the inhibition. The K_i values for enzyme inhibition were as low as 0.3nM and in general, these compounds were selective for CEs. Weaker inhibition of hAChE and hBChE was observed with the thioether-containing compounds; however in all cases where inhibition of the cholinesterases was seen, the influence on substrate turnover was limited. The most potent CE inhibitors (compound **1** for the 5 min assay and compound **6** for the 24 hr assay) demonstrated no inhibition of hAChE or hBChE at concentrations up to 100 μM (Tables 2 and 3). Also, the presence of the phenyl ring in the R group (compound **20**) significantly reduced the inhibitory potency of the molecules towards the cholinesterases as compared to the CEs. This observation is consistent with our previous studies using ethane-1,2-dione based inhibitors of esterases, which indicated that the hydrophobicity and aromaticity of the molecules significantly impacted their inhibitory potency towards esterases (Hyatt et al., 2005; Wadkins et al., 2005).

The hypothesis that increased hydrophobicity correlates with inhibitor potency has been corroborated with the studies described here, which indicate that compounds containing longer, more hydrophobic, alkyl chains are more potent inhibitors of CEs (C_{12} > C_{10} > C_8 > C_6 > C_4; Table 2, and Figure 2A). This trend is likely due to the fact that the active sites of these proteins exist as deep gorges within the enzymes that are lined with aromatic amino acids (Bencharit et al., 2002; Bencharit et al., 2003a; Bencharit et al., 2003b). As a consequence, this gorge is relatively

Molecular Pharmacology Fast Forward. Published on December 13, 2006 as DOI: 10.1124/mol.105.021683
This article has not been copyedited and formatted. The final version may differ from this version.

hydrophobic and hence provides a suitable milieu for localization of water intolerant domains. This effect is clearly reflected in the K_i data values (Table 2), the graphical plots (Figure 2) and the QSAR pseudoreceptor models (Figure 4). However, these correlations were only observed in short-term assays (5 min) and not after prolonged incubation of the inhibitor with the enzymes. This suggests that the alkyl group significantly impedes the binding of the thioether to the CE. While the longer alkyl chains may increase the molecules' inhibitory potency towards the CEs, they also significantly reduce water solubility. This is exemplified by the calculated water solubilities and the logP values for these compounds (Table 5). Since these parameters are correlated (i.e., molecules containing longer chain alkyl groups are more hydrophobic and generally less water soluble) relatively good correlation coefficients were observed with the K_i values (Figure 2 and Table 6). However, for the development of these inhibitors for practical uses, these physicochemical parameters will have to be taken into account to yield a compound that balances biological activity with bioavailability.

A comparison of the 5 min and 24 hr datasets demonstrated that dramatic differences in the ability of some of these TFK analogs to inhibit the CEs. For example, compounds **12** and **13** generated K_i values ranging from 9.8 – 79.5μM for the different CEs in the short term assays. However, following a 24 hr preincubation with enzyme, these same inhibitors yielded K_{iapp} values between 0.8 and 90nM (0.5 – 34.3nM using Eq. 2). This suggests that these compounds have very slow 'on' rates and that extended incubation times are required to achieve equilibrium

Molecular Pharmacology Fast Forward. Published on December 13, 2006 as DOI: 10.1124/mol.105.021683
This article has not been copyedited and formatted. The final version may differ from this version.

between enzyme and inhibitor. In contrast, compound **7** produced very low K_i values for all three CEs in the 5 min assay, yet after 24 hr preincubation, the K_{iapp} constants had increased over 1000- and 140-fold for hiCE and rCE, respectively. We envisage that for this inhibitor, the 'on' rate for enzyme is very high, but the 'off' rate is much slower. Hence initially, a very high concentration of EI is formed that cannot undergo substrate binding and hydrolysis. However, after prolonged incubation, the level of EI complex would reduce (due to the loss of the inhibitor from the enzyme) and at equilibrium, substrate hydrolysis would increase, indicated by a relatively larger K_i value.

A number of studies have examined the role of the sulfur atom beta to the carbonyl carbon in inhibitor potency. It has been well-established that inclusion of the sulfur atom increases inhibition of juvenile hormone esterases (Székács et al., 1992). However, the effects upon mammalian esterases have been less closely examined. A comparison of compound **8** and its analog compound **7** (in which the sulfur atom has been replaced by a methylene moiety) demonstrates an interesting result. For both human enzymes as well as rCE, the methylene analog (**7**) was a more potent inhibitor then the thioether-containing compound in the 5 min assays. However, following a 24 hr preincubation the converse is true. These results suggest that the established enzyme/inhibitor equilibrium is crucial for effective CE inhibition and indicate that the role of the sulfur atom significantly differs in mammalian and some insect esterases.

Molecular Pharmacology Fast Forward. Published on December 13, 2006 as DOI: 10.1124/mol.105.021683
This article has not been copyedited and formatted. The final version may differ from this version.

In general, the trend for inhibitor potency for a compound with a given alkyl chain length was on the order of thioether>sulfonyl>sulfinyl. The reasons for this are unclear. The data cannot be explained based upon the steric parameters of the sulfur, sulfoxide or the sulfone moieties. One possibility is that the sulfoxide-containing compounds are highly hydrated. It has been hypothesized that the ketone is the active form of the inhibitor (Wheelock et al., 2003), however it has also been reported that potent inhibitors exist as their hydrated forms in aqueous solution (Roe et al., 1997). If both of these reports are accurate, then the equilibrium between the ketone and *gem*-diol forms of the inhibitor must be sufficiently dynamic such that adequate concentrations of the ketone are available for enzyme inhibition. This theory is supported by the kinetic parameters of the sulfoxide-containing inhibitors, which were significantly slower than the corresponding sulfone or thioether analogs (Wheelock et al., 2002). The observation that increased enzyme/inhibitor incubation times increased the inhibition potency argues that effects upon ketone equilibrium are important for enzyme inhibition. However, it would be necessary to measure the binding constants of the individual sulfur oxidation states to fully test this hypothesis.

Analysis of the K_i values using the QSAR modeling program Quasar generated excellent observed versus predicted correlations (Figure 3), even with relatively small data sets. Since the derived q^2 values were significantly greater than 0.4, a value that is considered the cutoff for use of these models for predicting activity in biological systems (Lundstedt et al., 1998), it is likely that these models will have considerable predictive power in the design of novel TFK-based CE.

Molecular Pharmacology Fast Forward. Published on December 13, 2006 as DOI: 10.1124/mol.105.021683
This article has not been copyedited and formatted. The final version may differ from this version.

The derived pseudoreceptor models (Figure 4) were remarkably similar in structure to those obtained following CE enzyme inhibition studies performed with a series of benzil and sulfonamide analogs (Fleming et al., 2005; Wadkins et al., 2005; Wadkins et al., 2004). These models clearly reflect the charged amino acid residues that are present within the active site gorges of hiCE, hCE1 and rCE. However, as compared to the benzil pseudoreceptor models (Wadkins et al., 2005), the TFK models demonstrate greater similarity to each other for each enzyme. Consequently, the enzyme selectivity that is seen with some of the benzil analogs for the different mammalian CEs was not observed with the TFK compounds.

TFKs are slow, tight-binding inhibitors that can require significant time intervals to reach equilibrium (Wheelock et al., 2002). The kinetics of this process appears to be related to inhibitor structure and it is therefore likely that many of the inhibitors have not reached equilibrium in short-term assays. Therefore, we compared a relatively short assay time (5 min), with a more prolonged 24 hr preincubation period. Potent TFKs almost certainly exist as the *gem*-diol form in aqueous solution (Figure 1). Therefore, the rate and/or extent of the ketone/*gem*- diol equilibrium may affect inhibitor potency. Since previous work suggested that the active form of the inhibitor is the ketone (Wheelock et al., 2003), dehydration of the *gem*-diol must occur to enable the carbonyl carbon to be subjected to nucleophilic attack by the catalytic serine. However, this process is poorly understood and will require further investigation to elucidate the mechanism of TFK-mediated CE inhibition.

Molecular Pharmacology Fast Forward. Published on December 13, 2006 as DOI: 10.1124/mol.105.021683
This article has not been copyedited and formatted. The final version may differ from this version.

Overall, these studies have elucidated parameters (e.g. alkyl chain length) that are important for the biological activity of the TFK analogs and this information, used in conjunction with the 3-D pseudoreceptor models, should be beneficial in the design of novel inhibitors. Additionally, the models that were obtained from these studies were entirely consistent with those that have previously been described for the mammalian CEs (Wadkins et al., 2005; Wadkins et al., 2004). By comparison of these independent models, it is likely that subtle differences will be identified, allowing for the design of more selective and potentially more potent inhibitors. For example, a TFK-based inhibitor might combine the asymmetric trifluoropropan-2-one head group with a bulkier hydrophobic moiety. Compounds having large aromatic ring systems are excellent inhibitors of CEs (Hyatt et al., 2005; Wadkins et al., 2005), therefore, TFK analogs containing more bulky and/or aromatic moieties may become more potent inhibitors. Studies designed to assess the properties of such compounds are currently underway.

References

Ahmad S and Forgash AJ (1976) Nonoxidative enzymes in the metabolism of insecticides. *Ann Clin Biochem* **13**:141-164.

Ashour MB and Hammock BD (1987) Substituted trifluoroketones as potent, selective inhibitors of mammalian carboxylesterases. *Biochem Pharmacol* **36**:1869-1879.

Bencharit S, Morton CL, Howard-Williams EL, Danks MK, Potter PM and Redinbo MR (2002) Structural insights into CPT-11 activation by mammalian carboxylesterases. *Nat Struct Biol* **9**:337-342.

Bencharit S, Morton CL, Hyatt JL, Kuhn P, Danks MK, Potter PM and Redinbo MR (2003a) Crystal structure of human carboxylesterase 1 complexed with the Alzheimer's drug tacrine. From binding promiscuity to selective inhibition. *Chem & Biol* **10**:341-349.

Bencharit S, Morton CL, Xue Y, Potter PM and Redinbo MR (2003b) Structural basis of heroin and cocaine metabolism by a promiscuous human drug-processing enzyme. *Nat Struct Biol* **10**:349-356.

Brodbeck U, Schweikert K, Gentinetta R and Rottenberg M (1979) Fluorinated aldehydes and ketones acting as quasi-substrate inhibitors of acetylcholinesterase. *Biochim Biophys Acta* **567**:357-369.

Cashman J, Perroti B, Berkman C and Lin J (1996) Pharmacokinetics and molecular detoxification. *Environ Health Perspect* **104**:23-40.

Doctor BP, Toker L, Roth E and Silman I (1987) Microtiter assay for acetylcholinesterase. *Anal Biochem* **166**:399-403.

Fleming CD, Bencharit S, Edwards CC, Hyatt JL, Tsurkan L, Bai F, Fraga C, Morton CL, Howard-Williams EL, Potter PM and Redinbo MR (2005) Structural insights into drug processing by human carboxylesterase 1: tamoxifen, mevastatin, and inhibition by benzil. *J Mol Biol* **352**:165-177.

Hammock BD, Abdel-Aal AI, Mullin CA, Hanzlik TN and Roe RM (1984) Substituted thiotrifluoropropanones as potent selective inhibitors of juvenile hormone esterase. *Pestic Biochem Phys* **22**:209-223.

Hammock BD, Wing KD, Mclaughlin J, Lovell VM and Sparks TC (1982) Trifluoromethylketones as possible transition-state analog inhibitors of juvenile-hormone esterase. *Pesticide Biochem Physiol* **17**:76-88.

Hyatt JL, Stacy V, Wadkins RM, Yoon KJ, Wierdl M, Edwards CC, Zeller M, Hunter AD, Danks MK, Crundwell G and Potter PM (2005) Inhibition of carboxylesterases by benzil (diphenylethane-1,2-dione) and heterocyclic analogues is dependent upon the aromaticity of the ring and the flexibility of the dione moiety. *J Med Chem* **48**:5543-5550.

Jakalian A, Jack DB and Bayly CI (2002) Fast, efficient generation of high-quality atomic charges. AM1-BCC model: II. Parameterization and validation. *J Med Chem* **23**:1623-1641.

Kraulis PJ (1991) MOLSCRIPT: A program to produce both detailed and schematic plots of protein structures. *J Appl Cryst* **24**:946-950.

Linderman RJ, Upchurch L, Lonikar M, Venkatesh K and Roe RM (1989) Inhibition of insect juvenile-hormone esterase by alpha,beta-unsaturated and alpha-acetylenic trifluoromethyl ketones. *Pesticide Biochem Physiol* **35**:291-299.

Lundstedt T, Seifert E, Abramo L, Thelin B, Nystrom A, Pettersen J and Bergman B (1998) Experimental design and optimization. *Chemom Intell Lab Syst* **42**:3-40.

Merritt EA and Bacon DJ (1997) Raster 3D: Photorealistic molecular graphics. *Meth Enzymol* **277**:505-524.

Morrison JF and Walsh CT (1988) The behavior and significance of slow-binding enzyme inhibitors. *Adv in Enz* **61**:201-301.

Morton CL and Potter PM (2000) Comparison of *Escherichia coli, Saccharomyces cerevisiae, Pichia pastoris, Spodoptera frugiperda* and COS7 cells for recombinant gene expression: Application to a rabbit liver carboxylesterase. *Mol Biotechnol* **16**:193-202.

Morton CL, Wadkins RM, Danks MK and Potter PM (1999) CPT-11 is a potent inhibitor of acetylcholinesterase but is rapidly catalyzed to SN-38 by butyrylcholinesterase. *Cancer Res* **59**:1458-1463.

Munger JS, Shi GP, Mark EA, Chin DT, Gerard C and Chapman HA (1991) A serine esterase released by human alveolar macrophages is closely related to liver microsomal carboxylesterases. *J Biol Chem* **266**:18832-18838.

Potter PM, Pawlik CA, Morton CL, Naeve CW and Danks MK (1998) Isolation and partial characterization of a cDNA encoding a rabbit liver carboxylesterase that activates the prodrug Irinotecan (CPT-11). *Cancer Res* **52**:2646-2651.

Redinbo MR and Potter PM (2005) Mammalian Carboxylesterases: From drug targets to protein therapeutics. *Drug Discov Today* **10**:313-325.

Roe RM, Anspaugh DD, Venkatesh K, Linderman RJ and Graves DM (1997) A novel geminal diol as a highly specific and stable *in vivo* inhibitor of insect juvenile hormone esterase. *Arch Insect Biochem Physiol* **36**:165-179.

Rosell G, Herrero S and Guerrero A (1996) New trifluoromethyl ketones as potent inhibitors of esterases: ^{19}F NMR spectroscopy of transition state analog complexes and structure-activity relationships. *Biochem Biophys Res Comm* **226**:287-292.

Ross MK, Borazjani A, Edwards CC and Potter PM (2006) Hydrolytic metabolism of pyrethroids by human and other mammalian carboxylesterases. *Biochem Pharmacol* **71**:657-669.

Schwer H, Langmann T, Daig R, Becker A, Aslanidis C and Schmitz G (1997) Molecular cloning and characterization of a novel putative carboxylesterase, present in human intestine and liver. *Biochem Biophys Res Comm* **233**:117-120.

Stewart JJ (1990) MOPAC: a semiempirical molecular orbital program. *J Comput Aided Mol Des* **4**:1-105.

Székács A, Bordás B and Hammock BD (1992) Transition state analog enzyme inhibitors: Structure-activity relationships of trifluoromethyl ketones., in *Rational Approaches to Structure, Activity, and Ecotoxicology of Agrochemicals* (Draber W and Fujita T eds) pp 219-249, CRC Press, Boca Raton, Florida.

Vedani A and Dobler M (2002a) 5D-QSAR: the key for simulating induced fit? *J Med Chem* **45**:2139-2149.

Vedani A and Dobler M (2002b) Multidimensional QSAR: Moving from three- to five-dimensional concepts. *Quant Struct-Act Relat* **21**:382-390.

Vedani A, Dobler M and Lill MA (2005) Combining protein modeling and 6D-QSAR simulating the binding of structurally diverse ligands to the estrogen receptor. *J Med Chem* **48**:3700-3703.

Wadkins RM, Hyatt JL, Wei X, Yoon KJ, Wierdl M, Edwards CC, Morton CL, Obenauer JC, Damodaran K, Beroza P, Danks MK and Potter PM (2005) Identification and characterization of novel benzil (diphenylethane-1,2-dione) analogues as inhibitors of mammalian carboxylesterases. *J Med Chem* **48**:2905-2915.

Wadkins RM, Hyatt JL, Yoon KJ, Morton CL, Lee RE, Damodaran K, Beroza P, Danks MK and Potter PM (2004) Identification of novel selective human intestinal carboxylesterase inhibitors for the amelioration of irinotecan-induced diarrhea: Synthesis, quantitative structure-activity relationship analysis, and biological activity. *Mol Pharmacol* **65**:1336-1343.

Wadkins RM, Potter PM, Vladu B, Marty J, Mangold G, Weitman S, Manikumar G, Wani MC, Wall ME and Von_Hoff DD (1999) Water soluble 20(S)-glycinate esters of 10,11-methylenedioxycamptothecins are highly active against human breast cancer xenografts. *Cancer Res* **59**:3424-3428.

Webb JL (1963) *Enzyme and Metabolic Inhibitors. Volume 1. General Principles of Inhibition*. Academic Press Inc., New York.

Wheelock CE, Colvin ME, Uemura I, Olmstead MM, Sanborn JR, Nakagawa Y, Jones AD and Hammock BD (2002) Use of ab initio calculations to predict the biological potency of carboxylesterase inhibitors. *J Med Chem* **45**:5576-5593.

Wheelock CE, Nakagawa Y, Akamatsu M and Hammock BD (2003) Use of classical and 3-D QSAR to examine the hydration state of juvenile hormone esterase inhibitors. *Bioorg Med Chem* **11**:5101-5116.

Wheelock CE, Severson TF and Hammock BD (2001) Synthesis of new carboxylesterase inhibitors and evaluation of potency and water solubility. *Chem Res Toxicol* **14**:1563-1572.

Wheelock CE, Shan G and Ottea JA (2005) Overview of carboxylesterases and their role in metabolism of insecticides. *J Pestic Sci* **30**:75-83.

Molecular Pharmacology Fast Forward. Published on December 13, 2006 as DOI: 10.1124/mol.105.021683
This article has not been copyedited and formatted. The final version may differ from this version.

Footnotes

This work was supported in part by NIH grants CA76202, CA79763, CA98468, CA108775, a Cancer Center Core grant P30 CA21765, NIEHS Grant R37 ES02710, NIEHS Superfund Grant P42 ES04699, NIEHS Center for Environmental Health Sciences Grant P30 ES05707 and by the American Lebanese Syrian Associated Charities. C.E.W. was supported by a Japanese Society for the Promotion of Science (JSPS) post-doctoral fellowship and NIH post-doctoral training grant T32 DK07355-22. P.D.J. was supported by a NIH/NHLBI Ruth L. Kirschstein NRSA grant (F32 HL078096).

Molecular Pharmacology Fast Forward. Published on December 13, 2006 as DOI: 10.1124/mol.105.021683
This article has not been copyedited and formatted. The final version may differ from this version.

Legends for Schemes and Figures

Scheme 1. A schematic indicating the potential reaction mechanism for the formation of product (P) for the enzyme (E) / substrate (S) equilibrium in the presence of inhibitor (I). The constants α, β, K_s K_i and k are described in the text.

Figure 1. Inter-conversion of the ketone and the *gem*-diol forms of the inhibitors following hydration. The naming of the atoms is indicated by the Greek letters.

Figure 2. Correlation of K_i values for CE inhibition with length of the alkyl moiety (A), the ClogP of the inhibitor (B) or the water solubility of compounds **1**, **4**, **8**, **11** and **18**. In all graphs, data points and computer predicted curve fits are indicated in blue for hiCE, red for hCE1, and green for rCE. Goodness of fit coefficients (r^2) for the lines are indicated on the graphs.

Figure 3. Graphs of observed versus predicted K_i values for CE inhibition with the TFK analogs. The upper panel represents data points derived from the 5 min assays, and the lower panel from the 24 hr preincubation. Data depicted in black represent those used to define the QSAR models, and the validation sets are shown in red.

Figure 4. Pseudoreceptor models that describe the best fits for the inhibition data sets derived from the 24hr preincubation assays for the TFK inhibitors. The models for hiCE (A), hCE1 (B), and rCE (C) are depicted as colored spheres on a

Molecular Pharmacology Fast Forward. Published on December 13, 2006 as DOI: 10.1124/mol.105.021683
This article has not been copyedited and formatted. The final version may differ from this version.

hydrophobic gray grid. Areas that are hydrophobic are indicated in gray, whereas blue spheres represent areas that are positively charged (+0.1*e*) and light blue spheres correspond to hydrogen bond donors. Orange-red spheres represent areas that are negatively charged (-0.1*e*), while orange spheres indicate hydrogen bond acceptors. In all cases, *e* is the charge of the proton. The structure of compound **4** is shown in black and the figure was generated using Molscript (Kraulis, 1991) and Raster3D (Merritt and Bacon, 1997).

Molecular Pharmacology Fast Forward. Published on December 13, 2006 as DOI: 10.1124/mol.105.021683
This article has not been copyedited and formatted. The final version may differ from this version.

Table 1. ID, structure and names of the compounds assayed

ID	Structure[a]	Name
1	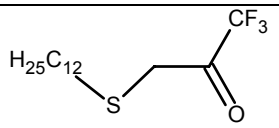	3-(Dodecylthio)-1,1,1-trifluoropropan-2-one
2	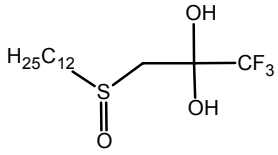	3-(Dodecylsulfinyl)-1,1,1-trifluoropropane-2,2-diol
3	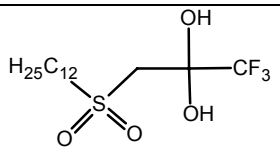	3-(Dodecylsulfonyl)-1,1,1-trifluoropropane-2,2-diol
4	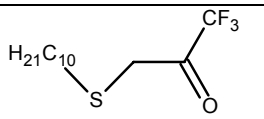	3-(Decylthio)-1,1,1-trifluoropropan-2-one
5	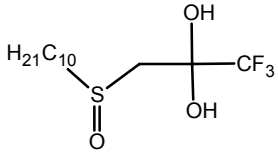	3-(Decylsulfinyl)-1,1,1-trifluoropropane-2,2-diol
6	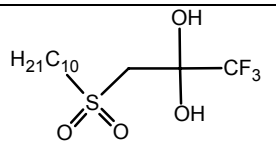	3-(Decylsulfonyl)-1,1,1-trifluoropropane-2,2-diol
7	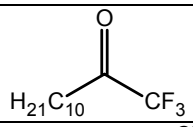	1,1,1-Trifluorododecan-2-one
8	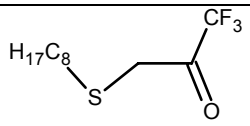	1,1,1-Trifluoro-3-(octylthio)propan-2-one
9	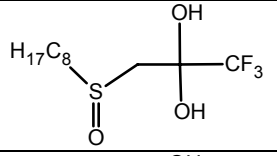	1,1,1-Trifluoro-3-(octylsulfinyl)propane-2,2-diol
10	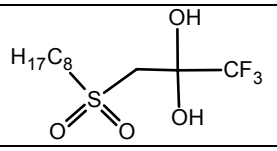	1,1,1-Trifluoro-3-(octylsulfonyl)propane-2,2-diol

Molecular Pharmacology Fast Forward. Published on December 13, 2006 as DOI: 10.1124/mol.105.021683
This article has not been copyedited and formatted. The final version may differ from this version.

11	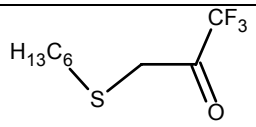	1,1,1-Trifluoro-3-(hexylthio)propan-2-one
12	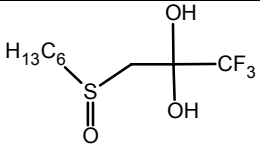	1,1,1-Trifluoro-3-(hexylsulfinyl)propane-2,2-diol
13	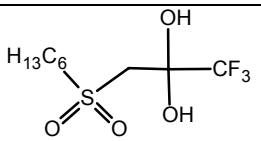	1,1,1-Trifluoro-3-(hexylsulfonyl)propane-2,2-diol
14	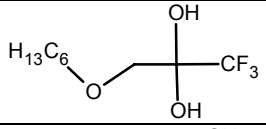	1,1,1-Trifluoro-3-(hexyloxy)propane-2,2-diol
15	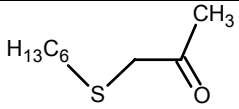	1-(Hexylthio)propan-2-one
16	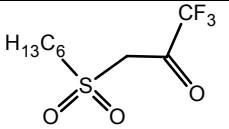	1-(Hexylsulfonyl)propan-2-one
17	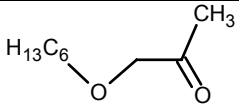	1-(Hexyloxy)propan-2-one
18	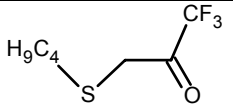	3-(Butylthio)-1,1,1-trifluoropropan-2-one
19	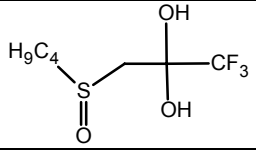	3-(Butylsulfinyl)-1,1,1-trifluoropropane-2.2-diol
20	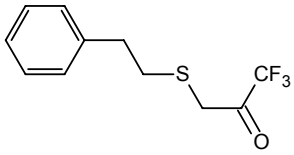	1,1,1-Trifluoro-3-(phenethylthio)propan-2-one
21	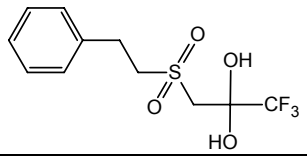	1,1,1-Trifluoro-3-phenethylsulfonyl) propane-2,2-diol

[a] – Compounds are drawn in either their ketone or *gem*-diol form dependent upon the chemical structure obtained from ^{1}H NMR spectroscopy in $CDCl_3$. Displayed structures were used for the QSAR molecular modeling.

Molecular Pharmacology Fast Forward. Published on December 13, 2006 as DOI: 10.1124/mol.105.021683
This article has not been copyedited and formatted. The final version may differ from this version.

Table 2. K_i values for the inhibition of hiCE, hCE1, rCE, hAChE or hBChE following preincubation of the enzymes with the TFK analogs for 5 min. Data were analyzed using Eq. 1.

ID	K_i value for indicated enzyme ± SE (nM) [Mode of enzyme inhibition][a]				
	hiCE	hCE1	rCE	hAChE	hBChE
1	15.0 ± 2.0 [c][a]	71.0 ± 7.0 [pnc][a]	160 ± 20 [pnc]	>100,000	1,200 ± 300 [pc][a]
2	54.0 ± 6.0 [pc]	1,900 ± 300 [pnc]	1,100 ± 200 [pnc]	>100,000	>100,000
3	32.0 ± 2.0 [pc]	740 ± 100 [pnc]	150 ± 20 [c]	>100,000	>100,000
4	150 ± 20 [pnc]	130 ± 20 [pnc]	160 ± 30 [pnc]	710 ± 110 [pc]	10,800 ± 1,500 [pnc]
5	1,900 ± 300 [pnc]	5,300 ± 100 [pnc]	2,500 ± 200 [pnc]	>100,000	>100,000
6	80.0 ± 5.0 [c]	800 ± 130 [pnc]	220 ± 20 [c]	>100,000	>100,000
7	22 ± 1 [pc]	150 ± 20 [pnc]	140 ± 10 [pnc]	>100,000	3,800 ± 440 [pc]
8	220 ± 40 [pnc]	190 ± 40 [pnc]	150 ± 30 [pnc]	1,750 ± 220 [pc]	11,500 ± 1,100 [pnc]
9	2,400 ± 700 [pnc]	14,700 ± 2,900 [pnc]	4,900 ± 1,400 [pnc]	>100,000	>100,000
10	4,700 ± 5000 [pnc]	1,500 ± 300 [pnc]	4,800 ± 800 [pnc]	>100,000	>100,000

Molecular Pharmacology Fast Forward. Published on December 13, 2006 as DOI: 10.1124/mol.105.021683
This article has not been copyedited and formatted. The final version may differ from this version.

11	560 ± 110 [pnc]	330 ± 80 [pnc]	250 ± 50 [pnc]	>100,000	18,400 ± 2,900 [pc]
12	67,900 ± 35,90 [pnc]	79,500 ± 3,200 [pnc]	22,800 ± 12,400 [pnc]	>100,000	>100,000
13	27,500 ± 5,800 [pnc]	9,800 ± 1,400 [pnc]	15,300 ± 1,800 [pnc]	>100,000	>100,000
14	9,100 ± 1,600 [pnc]	3,300 ± 1,000 [pnc]	2,700 ± 800 [pnc]	>100,000	>100,000
15	>100,000	>100,000	>100,000	>100,000	>100,000
16	>100,000	>100,000	>100,000	>100,000	>100,000
17	>100,000	>100,000	>100,000	>100,000	>100,000
18	1,700 ± 300 [pnc]	800 ± 100 [pnc]	420 ± 50 [pnc]	2,500 ± 100 [pc]	>100,000
19	>100,000	>100,000	>100,000	>100,000	>100,000
20	750 ± 90 [pnc]	120 ± 20 [pc]	410 ± 110 [pnc]	72,000 ± 37,000 [pnc]	65,600 ± 8,000 [pnc]
21	50,700 ± 13,600 [pnc]	13,800 ± 3,000 [pnc]	13,600 ± 2,300 [pnc]	>100,000	>100,000

[a] – Modes of enzyme inhibition are: [c] – competitive; [pc] – partially competitive; [pnc] – partially non-competitive.

Molecular Pharmacology Fast Forward. Published on December 13, 2006 as DOI: 10.1124/mol.105.021683
This article has not been copyedited and formatted. The final version may differ from this version.

Table 3. K_i values for the inhibition of hiCE, hCE1, rCE, hAChE or hBChE following preincubation of the enzymes with the TFK analogs for 24 hr. Data were analyzed using Eq. 1.

ID	K_{iapp} value for indicated enzyme ± SE (nM) [Mode of enzyme inhibition][a]				
	hiCE	hCE1	rCE	hAChE	hBChE
1	64.9 ± 22.2 [pnc][a]	24.7 ± 5.0 [pnc]	46.7 ± 12.9 [pnc]	>100,000	2,550 ± 310 [pc][a]
2	4.50 ± 1.10 [pnc]	0.44 ± 0.08 [pc]	1.10 ± 0.11 [pc]	>100,000	>100,000
3	0.84 ± 0.17 [pc]	0.36 ± 0.05 [c][a]	0.66 ± 0.06 [pc]	>100,000	>100,000
4	59.2 ± 17.5 [pnc]	11.3 ± 3.0 [pnc]	29.0 ± 4.0 [pnc]	16,200 ± 3,300 [pnc]	95,000 ± 6,700 [pnc]
5	6.60 ± 0.87 [pnc]	0.49 ± 0.08 [c]	16.1 ± 1.4 [pnc]	>100,000	>100,000
6	0.75 ± 0.17 [pc]	0.86 ± 0.20 [pnc]	1.35 ± 0.10 [pc]	>100,000	>100,000
7	25,200 ± 2,100 [pnc]	6.50 ± 0.64 [nc]	20,500 ± 3,800 [pnc]	>100,000	>100,000
8	3.60 ± 0.64 [pc]	4.24 ± 0.81 [pc]	42.6 ± 5.2 [pnc]	1,630 ± 500 [pc]	40,400 ± 5,100 [pnc]
9	4.90 ± 0.89 [pnc]	1.22 ± 0.10 [pc]	4.70 ± 0.54 [pc]	>100,000	>100,000
10	33.0 ± 7.5 [pnc]	0.59 ± 0.10 [c]	22.8 ± 3.4 [pnc]	>100,000	>100,000

Molecular Pharmacology Fast Forward. Published on December 13, 2006 as DOI: 10.1124/mol.105.021683
This article has not been copyedited and formatted. The final version may differ from this version.

11	67.7 ± 10.1 [pnc]	14.1 ± 2.8 [nc]	10.1 ± 1.1 [c]	>100,000	>100,000
12	0.79 ± 0.05 [pc]	3.50 ± 0.30 [pc]	89.8 ± 11.8 [pnc]	>100,000	>100,000
13	3.0 ± 0.3 [pc]	2.36 ± 0.26 [pnc]	19.5 ± 3.1 [pc]	>100,000	>100,000
14	1.20 ± 0.16 [pc]	2.65 ± 0.45 [pnc]	11.3 ± 0.8 [nc][a]	>100,000	>100,000
15	>100,000	>100,000	>100,000	>100,000	>100,000
16	450 ± 100 [pc]	3,610 ± 1,600 [pnc]	18,300 ± 3,900 [pnc]	>100,000	>100,000
17	>100,000	>100,000	>100,000	>100,000	>100,000
18	17.0 ± 2.0 [pc]	13.5 ± 2.2 [pnc]	45.8 ± 8.8 [pnc]	31,400 ± 7,500 [pnc]	>100,000
19	0.20 ± 0.09 [pc]	32.9 ± 8.0 [pnc]	268 ± 30 [pnc]	>100,000	>100,000
20	62.1 ± 10.4 [pnc]	16.9 ± 4.2 [nc]	42.4 ± 7.7 [pnc]	360 ± 35 [pc]	>100,000
21	376 ± 77 [pnc]	4.70 ± 0.37 [pnc]	29.9 ± 10.7 [pnc]	>100,000	>100,000

[a] - Modes of enzyme inhibition are: [c] – competitive; [nc] – non-competitive; [pc] – partially competitive; [pnc] – partially non-competitive.

Molecular Pharmacology Fast Forward. Published on December 13, 2006 as DOI: 10.1124/mol.105.021683
This article has not been copyedited and formatted. The final version may differ from this version.

Table 4. K_i values for the inhibition of hiCE, hCE1 or rCE following preincubation of the enzymes with the TFK analogs for 24 hr. Datasets were analyzed using the model applicable for slow binding inhibitors (Eq.2).

ID	K_i value for indicated enzyme ± SE (nM)		
	hiCE	hCE1	rCE
1	5.4 ± 1.9	7.4 ± 1.5	3.3 ± 1.0
2	0.4 ± 0.1	0.4 ± 0.1	1.4 ± 0.2
3	1.0 ± 0.2	0.4 ± 0.1	0.7 ± 0.1
4	4.6 ± 1.2	4.0 ± 0.9	2.8 ± 0.4
5	0.5 ± 0.1	0.5 ± 0.1	3.0 ± 0.3
6	1.1 ± 0.3	0.3 ± 0.1	1.6 ± 0.2
7	2,043.3 ± 146.8	2.3 ± 0.2	3,236.6 ± 271.1
8	3.50 ± 0.6	4.2 ± 0.9	7.8 ± 0.9
9	0.5 ± 0.1	0.6 ± 0.1	6.4 ± 1.1
10	5.8 ± 1.7	0.6 ± 0.1	36.8 ± 7.8
11	6.5 ± 0.9	5.2 ± 1.1	9.9 ± 1.3
12	0.5 ± 0.2	3.3 ± 0.3	21.7 ± 3.4
13	3.7 ± 0.7	0.7 ± 0.1	34.3 ± 7.6
14	1.2 ± 0.2	1.0 ± 0.2	1.7 ± 0.1
15	>100,000	>100,000	>100,000
16	577.9 ± 89.2	1,840.8 ± 560.3	2,516.3 ± 229.8
17	>100,000	>100,000	>100,000
18	16.5 ± 1.9	5.4 ± 0.7	7.7 ± 1.2
19	2.0 ± 0.6	14.3 ± 4.2	137.3 ± 34.2
20	4.8 ± 0.9	6.4 ± 1.8	5.5 ± 0.8
21	116.2 ± 37.4	6.0 ± 1.3	106.4 ± 32.0

Molecular Pharmacology Fast Forward. Published on December 13, 2006 as DOI: 10.1124/mol.105.021683
This article has not been copyedited and formatted. The final version may differ from this version.

Table 5. Predicted logP values and water solubilities for the thioether TFKs.

Compound	logP	Water solubility (mg/ml)
1	6.11	0.124
4	5.78	0.129
8	5.02	0.193
11	4.09	0.424
18	3.12	1.22

Molecular Pharmacology Fast Forward. Published on December 13, 2006 as DOI: 10.1124/mol.105.021683
This article has not been copyedited and formatted. The final version may differ from this version.

Table 6. Correlation coefficients for the TFK CE QSAR models.

Enzyme	Time	Observed versus predicted K_i (K_{iapp}) values (r^2)	Cross correlation coefficient (q^2)	q^2/r^2
hiCE	5 min	0.908	0.900	0.991
hCE1	5 min	0.943	0.896	0.950
rCE	5 min	0.948	0.900	0.949
hiCE	24 hr	0.941	0.900	0.956
hCE1	24 hr	0.935	0.900	0.963
rCE	24 hr	0.937	0.900	0.961

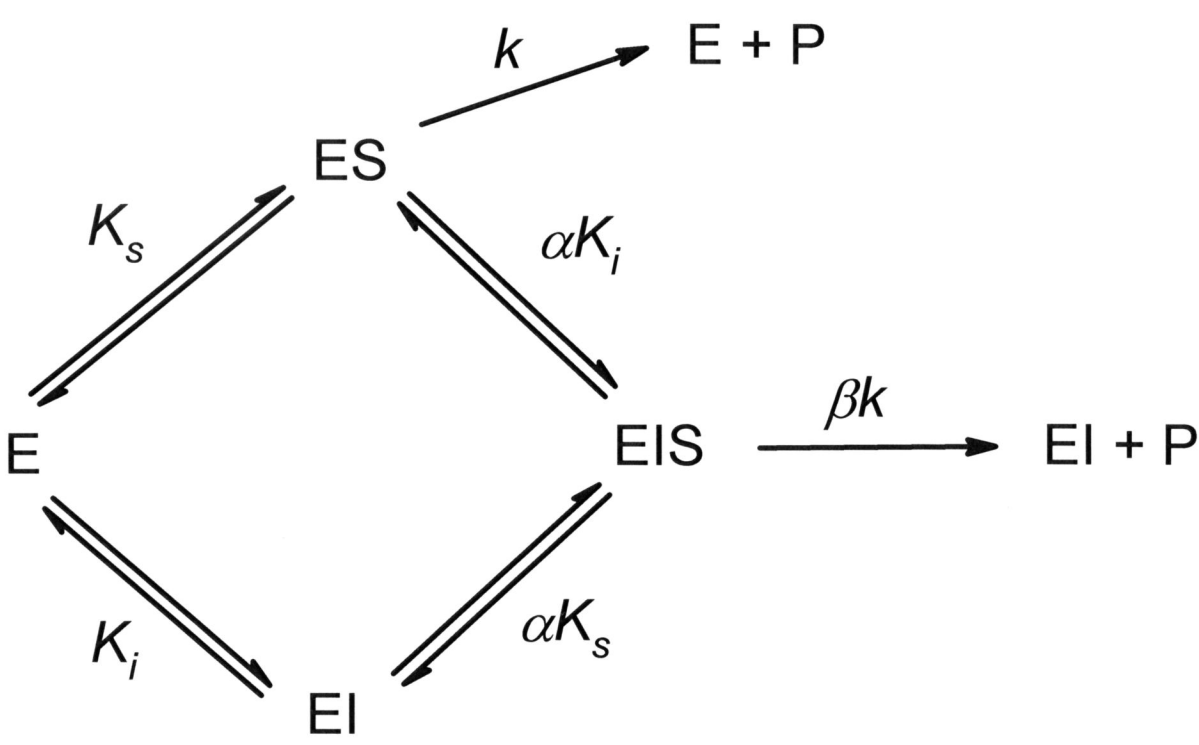
k
E + P
ES
K_s
αK_i
E
EIS
βk
EI + P
K_i
αK_s
EI

Figure 1

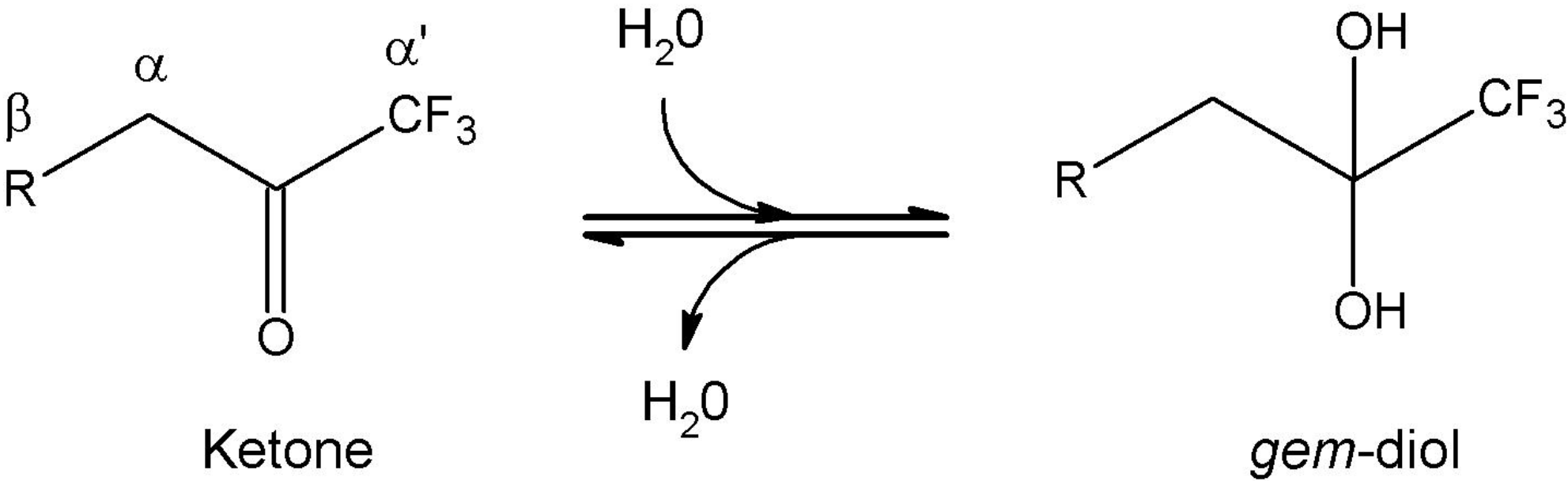

Figure 2

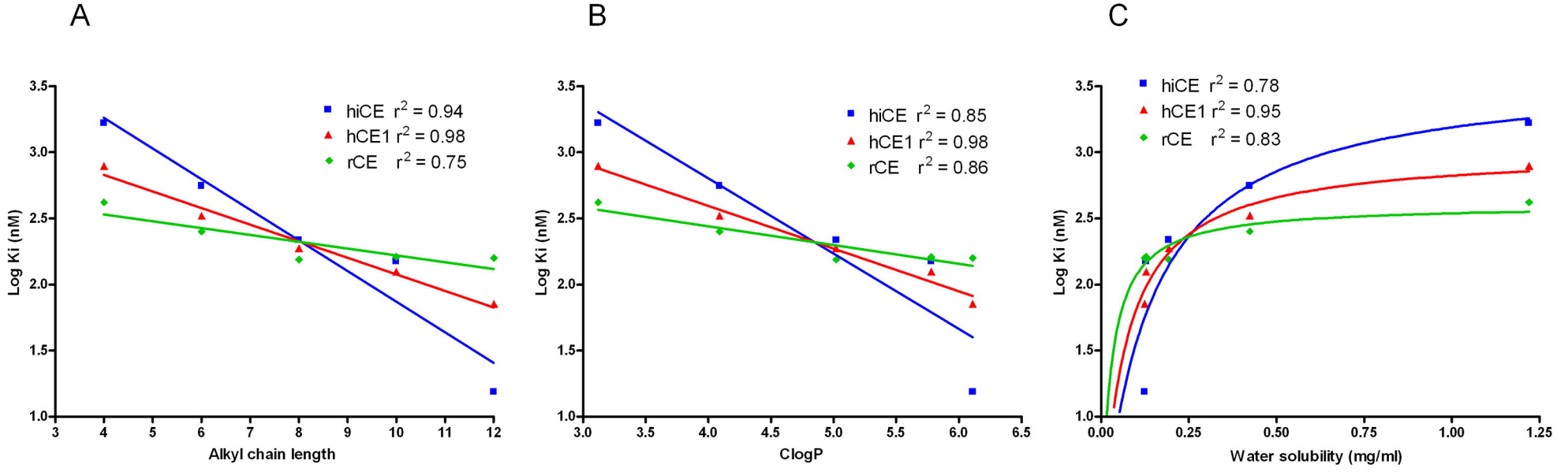
A
hiCE r2 = 0.94
hCE1 r2 = 0.98
rCE r2 = 0.75
Log Ki (nM)
Alkyl chain length
B
hiCE r2 = 0.85
hCE1 r2 = 0.98
rCE r2 = 0.86
Log Ki (nM)
ClogP
C
hiCE r2 = 0.78
hCE1 r2 = 0.95
rCE r2 = 0.83
Log Ki (nM)
Water solubility (mg/ml)

Figure 3

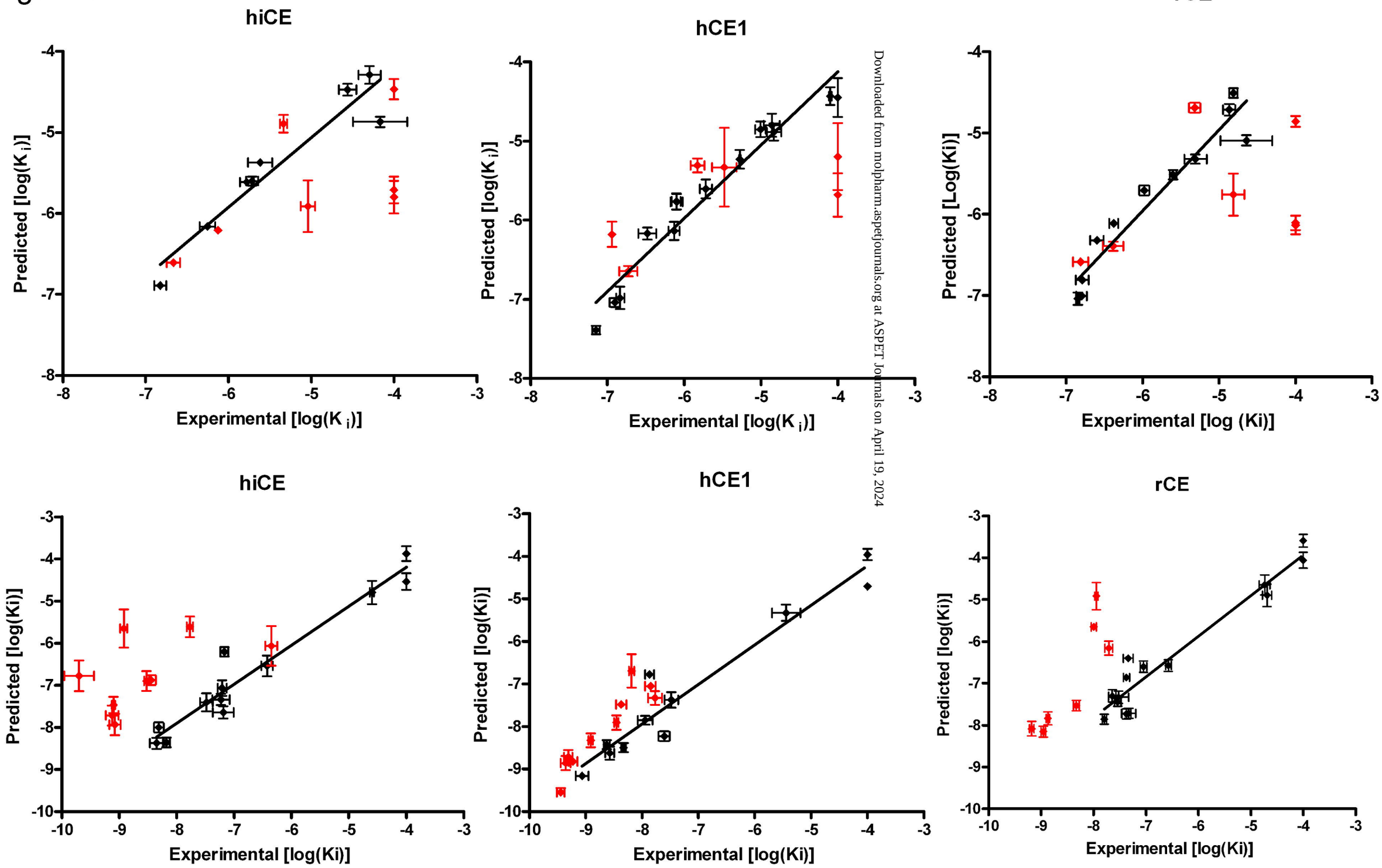

Figure 4